Tellus (1983), *35A*, 161–172

Stability properties of cylindrically curved mean flows

By RICHARD GROTJAHN, *Department of Land, Air and Water Resources, University of California, Davis CA 95616, U.S.A.*

(Manuscript received June 4; in final form September 20, 1982)

ABSTRACT

This article describes results from numerical experiments which isolate the influence of horizontal curvature upon various linear properties of growing baroclinic eddies. Cylindrically symmetric mean flows on an f-plane are studied; they have either strong or weak curvature. The radius of curvature is twice as large for weak as it is for strong curvature. Strong curvature reduces the growth rates and this is most evident only for the short waves. The baroclinic energy conversion is positive (from mean flow to eddy) and little influenced by curvature. The barotropic conversion is made more negative by stronger curvature; it is responsible for the growth rate reductions. The regions of positive and negative barotropic conversion are distributed about the mean flow jet in such a way that the eddies are tending to straighten out that jet. These results compare favorably with some previous analyses of long-wave flows by others.

1. Introduction

Synoptic scale cyclonic eddies are observed to develop in geophysical flows that have complex three-dimensional structure. Direct study of developing eddies in such complex time-mean flows is both mathematically and conceptually difficult. Preliminary to such a study, it seems reasonable to isolate and consider simpler components of the problem. It is hoped that results for the simpler component problems can be fruitfully used to comprehend the behavior of eddies in the more complex flows. It is suggested that the local environment in which the eddy evolves be classified according to three categories: (1) some measure of the local wind direction, (2) some measure of the local vertical shear (this includes turning of the wind with height) and (3) some measure of the local horizontal shear (this includes curvature of the flow). Category one isolates the Coriolis effect, category two emphasizes "baroclinic" processes and category three emphasizes "barotropic" processes. The separation of categories two and three may not be physically meaningful but it is traditional and often mathematically simpler. Diabatic effects, such as moisture processes, are not considered here. These processes may be important, but to date results from modeling attempts have been equivocal.

This is the third in a series of papers isolating effects of various properties of a time-mean flow upon linearly developing eddies. Each paper considers a problem in one of the three categories above; this paper considers curvature. In Grotjahn (1981), a unidirectional mean flow without horizontal variation but with differing compass orientation was investigated. In Grotjahn (1982) the direction of the mean flow was allowed to vary with height; again there was no other horizontal variation of the mean flow. The compass orientation was varied as well, to examine the relative magnitude of the variation caused by the Coriolis terms versus that due to the turning. Conservation of quasi-geostrophic potential vorticity was the equation for the interior of the domain in both eigenvalue problems.

The results from the two earlier papers in this series bear upon this study in the following ways. The direction of the mean flow on a β-plane (where the Coriolis parameter varies linearly) strongly influences many properties of the plane-wave solutions. Strong turning of the wind is needed to produce changes of similar magnitude. The vertical structure (of the eddy pressure field) seems rather insensitive to changes in orientation or turning despite quite different profiles of basic state potential vorticity gradient. This partly results from smoothing by the Poisson operator relating the pressure and potential vorticity fields. This suggests that the solution found for a judiciously chosen straight flow field would make a good guess for the solution derived and balanced for an environment that varies in three dimensions. This conclusion was employed in the work described below.

In this study an attempt is made to isolate the effects of curvature in the ambient wind field upon growing cyclone-scale eddies. This is accomplished by examining mean flows that are cylindrically symmetric, with variation in the vertical and radial dimensions. The vertical structure is the same as in the two antecedent articles. Radial variation is employed because: (1) it is observed in nature and (2) it provides a cross-flow length scale in the solutions. The radial shear is chosen so that the radial and longitudinal length scales are more or less equal. Directional effects from the rotating coordinate system are excluded by using a constant Coriolis parameter in this model. (This "f-plane" also simplifies the solution procedure.) This problem is nonseparable; while eigenvalue methods could still be employed, an initial value model, described in the next section, is used instead. The initial value model has several advantages over the eigenvalue approach. Its main disadvantage (how are the initial values chosen?) is satisfactorily resolved by noting the relative insensitivity of the eddy structure to the mean flow properties and using eigensolutions from similar straight-flow problems to derive the initial eddy fields.

There have been several previous studies that relate, in part, to the influence of curvature upon instability. Especially popular are studies of the stability of a long wave to small perturbations. Egger (1969), Lorenz (1972), Hoskins (1973), Gill (1974), Baines (1976) and Coacker (1977) all examined the stability of "barotropic" long waves. "Baroclinic" long waves have been included in studies by Frederiksen (1978), Kim (1978) and Niehaus (1980) to name a few representative examples. Since curvature was not specifically isolated, its effect upon the properties of eddies is difficult to discern from their work.

The author is aware of only one study (Drazin, 1978) where the influence of curvature was isolated. Drazin compared the neutral stability curves calculated when the Eady (1949) problem is formulated in Cartesian and (approximately) cylindrical coordinates. The results implied that curvature destabilizes the flow. The results presented in Section 3 will indicate the opposite. The apparent contradiction is resolved when the role played by the radial shear is considered. The radial shear barotropically stabilizes the eddies. The stabilization increases with stronger curvature and influences the shorter waves most. This effect dominates any destabilization caused by the curvature of the flow even for the modest radial shears examined here. There is no radial shear in Drazin's model.

2. Model description

The basis equations used in this study are similar to the basis equations used in earlier articles of this series. In the earlier papers, the equations are made separable and are solved as eigenvalue problems after assuming a wave-like solution in the horizontal and time dimensions. For the cylindrical flows examined here, the basis equations are nonseparable. Eigenvalue methods could still be employed for these equations, but such methods require the calculation (and storage) of many solutions, most of which are not of interest. The storage requirements are so great that the spatial resolution is severely limited by the size of the available computer. Even the large computers at the National Center for Atmospheric Research (NCAR), where the calculations were performed, are only marginally adequate. Instead, a high resolution prognostic (initial value) model is used. One solution can be easily focussed upon by a judicious choice of the initial conditions without requiring an excessive amount of storage. The initial conditions are defined from the solutions obtained for similar but separable eigenvalue problems, namely where the basic flow has the same vertical structure as here but is straight and without horizontal shear. This procedure has worked well on an f-plane for all the flows and eddy wavelengths examined thus far. The eddies require an initial period of time to adjust their structure, but soon converge to a fixed structure (within a few hundred time steps). The results presented below are based upon their asymptotic properties.

The quasi-geostrophic potential vorticity, Q, is defined as a three-dimensional Poisson operation upon the pressure field Φ. Hence:

$$Q = \varepsilon\Phi_{zz} + (\Omega\varepsilon + \varepsilon_z)\Phi_z + \Phi_{xx} + \Phi_{yy}.$$

(The Appendix annotates a list of symbols.) The parameter ε is inversely proportional to the static stability; Ω arises from allowing compressibility. Both ε and Ω are nondimensional functions of height only, are derived from representative mid-latitude atmospheric values and are graphed in Fig. 1.

The basis equations are conservation of quasi-geostrophic potential vorticity in the interior of the domain subject to several boundary conditions. As before, the equations are nondimensionalized by scaling for midlatitude traveling wave cyclones. Representative dimensional values are given in Grotjahn (1979); some examples are: $U = 1$ corresponds to 22 m s^{-1}, $J = 2.0$ corresponds to a wavelength of 4800 km at the radius R. The equations are linearized about a basic state (indicated by the overbar) that is cylindrically symmetric and fixed in time. The interior equation can be written as

$$q_t + \bar{U}q_x + \bar{V}q_y - \Phi_y\bar{q}_x + \Phi_x\bar{q}_y + \beta\Phi_x = 0. \quad (1)$$

The vertical coordinate used is height. Several terms are eliminated in (1) by assuming that the basic state advection of basic state potential vorticity is balanced by a forcing, F. Hence,

$$F = \bar{U}\bar{q}_x + \bar{V}\bar{q}_y + \beta\bar{V}.$$

This procedure is fairly standard in analyses of this type (e.g., Grotjahn, 1980, p. 190).

The horizontal and vertical variation of the basic flow ($\bar{U}$, $\bar{V}$) are separable. Their vertical profile $U(z)$ is shown in Fig. 1. The prescribed basic flow is zero at the bottom surface and reaches a maximum near the model's tropopause. In the horizontal, the velocity magnitude is maximum at radius R; it is nearly zero at the center and at large radius. These velocities are geostrophically derived from a basic pressure field which is defined as

$$P = U(z)\tanh(1.7\,\Lambda(r - R)), \quad (2)$$

where, as before,[1]

$$U(z) = 1.8\,\{1.0 - \tanh^2(z - 1.0) - \omega\exp(-0.1z)\}$$

and

$$\omega = 1.0 - \tanh^2(1.0).$$

Λ is a parameter that distinguishes the low from the high curvature experiments. This is discussed in detail at the beginning of the next section. It is natural to use a cylindrical coordinate system (r, θ) in the horizontal (x, y) dimensions. The radius (r) is directed outward from the center point where $x = 0$ and $y = 0$. The longitude angle (θ) is measured positive, counter clockwise from the line $x = 0$, $y > 0$. In this cylindrical coordinate system the basic state is independent of θ. This describes a basic state with a cylindrically symmetric low pressure center; its horizontal structure is shown in Fig. 2. We will discuss solutions for a low center; the solutions are mirror images for a high pressure center on an f-plane.

The boundary conditions chosen are: (a) vanishing vertical velocity at the top and bottom of the domain and (b) periodicity in x and y. The top and bottom boundary conditions can be written as

$$\phi_{zt} + \bar{U}\phi_{zx} + \bar{V}\phi_{zy} - \phi_y\overline{V_z} - \phi_x\overline{U_z} = 0 \quad \text{at } z = 0.5. \quad (3)$$

The top boundary is placed at a high altitude (scaled as 50 km) and plays little role for the

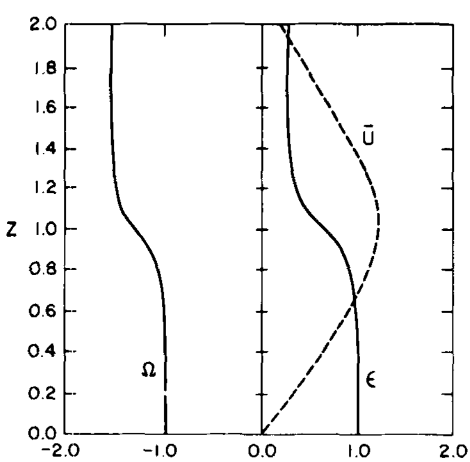

Fig. 1. Vertical profiles of ε, Ω and $U(z)$ where z is scaled by 10 m.

[1] Note the typographical error in this relationship as it appears in Grotjahn (1982).

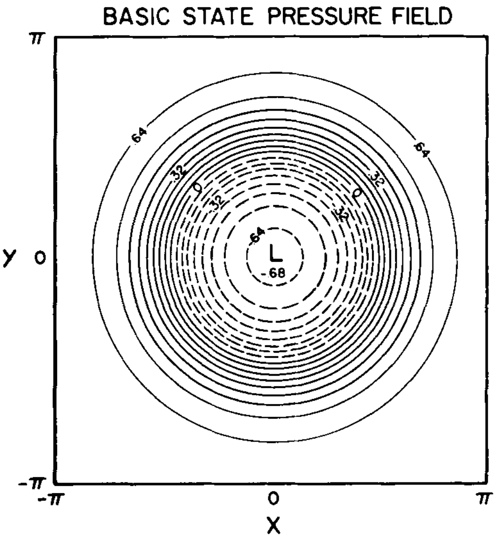

Fig. 2. Basic state pressure field horizontal structure. There is cylindrical symmetry and radial shear. The strongest gradient occurs at radius R.

solutions examined in this problem because of compressibility. This same boundary condition is used and discussed in the previous articles of this series. Doubly periodic horizontal boundary conditions are convenient to use in the spectral transform model described next. The horizontal boundaries are placed where the perturbation amplitude and basic flow are very small in amplitude. Accordingly, the periodic boundaries have no apparent influence upon the f-plane solutions. These boundary conditions do influence the solutions on a β-plane; those solutions are not described in this report.

The eqs. (1) and (3) were solved using a linear spectral numerical model. Plane geometry was used and the spectral functions are sines and cosines. Terms where two horizontally variant fields are multiplied were evaluated by transforming to grid points, performing the multiplication, then transforming back to phase space. Most of the integrations were performed using 11 levels and 21 wave numbers in each horizontal direction. This resolution appeared to be quite adequate based upon corresponding high resolution integrations that used 21 vertical levels and as many as 47 wave numbers. The vertical spacing of the levels is stretched providing high resolution in the troposphere and lower resolution at high altitudes. The stretching exponentially increases with height making the spacing approximately equivalent to equal increments of pressure between levels.

The eddy field in the numerical model is initialized by the following means. The eddy is assigned wavenumber N, such that its wavelength multiplied by N equals $2\pi R$. In the radial direction the eddies have largest amplitude at $r = R$ and decay exponentially for larger or smaller r. The vertical structure, comprising amplitude and phase of the eddies, is derived from solutions obtained in Grotjahn (1980) for straight basic flows that have the same vertical structure, but no horizontal variation. Hence:

$$\phi = \mathrm{Re}\,\{p(z)\exp\,(-b(r-R)^2 + iN\theta)\} \tag{4}$$

initially, where p is generally complex. The parameter b is positive and roughly proportional to N so that the eddies have comparable r and θ length scales. An example initial condition is depicted in Fig. 3.

3. Results and interpretation

In this section, the results are divided into two main categories. Low curvature ($\Lambda = 2.0$) and high curvature ($\Lambda = 1.0$) experiments are discussed. In the low curvature experiments the radius of maximum flow, R, is twice as large as for the high curvature experiments, while the horizontal and vertical structure is otherwise identical. Keeping an integer number ($N = n\Lambda$) of waves around the circle of radius R restricts the number of wavenumbers that can be examined, if only that integer is varied. Extra wavenumbers can be obtained by varying a horizontal scaling parameter, a, that manipulates the nondimensionalization of the equations. J, the (dimensionally scaled) longitudinal wave number, can be expressed as

$$J = an\Lambda.$$

a is varied from 0.21 to 0.27 in the calculation of the low curvature solutions and from 0.42 to 0.54 in the high curvature solutions. N equals $n\Lambda$, where n is 4, 5 or 6 and Λ is 1.0 (2.0) for the high (low) curvature cases. As can be seen, there is a compensation between the values of a and Λ for the high and low curvature cases to facilitate comparison of solutions with equivalent wavenumbers.

The wavenumber J relates the horizontal scaling used in the nondimensionalization to the dimensional circumference of the circle of radius R.

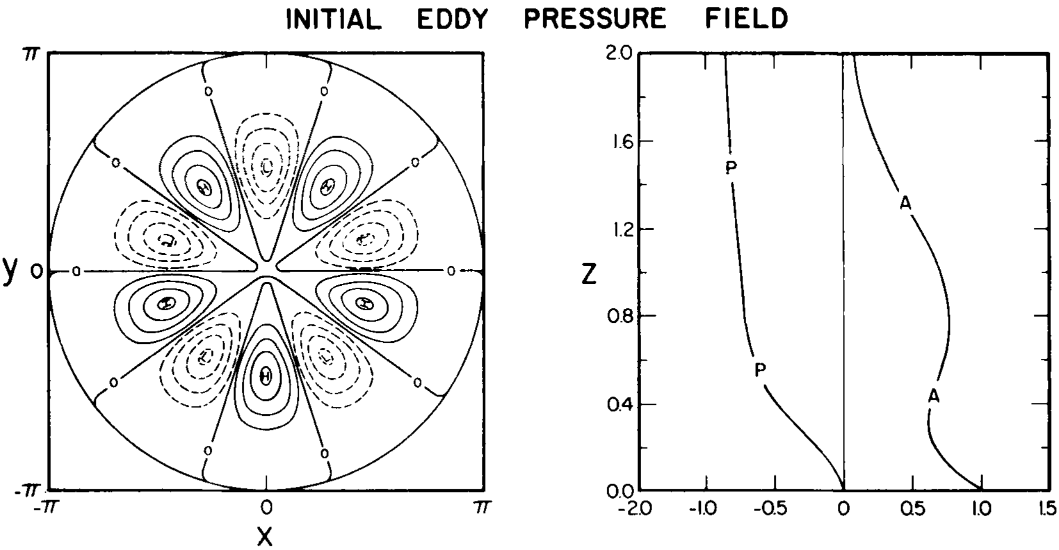

Fig. 3. Typical structure of the initial guess eddy fields; at left is the horizontal structure, where the eddies are centered about radius R; at right is the vertical structure where A is the eddy amplitude and P is one-half of the phase angle. The example shown is for $n = 5$, $\Lambda = 1.0$ and $a = 0.52$ so that $J = 2.6$.

Unlike N, J can be related to wavenumbers employed in previous stability analyses of straight flows. The short wave cut-off found by Eady (1949) roughly corresponds to $J = 2.4$. The α used in the previous papers of this series approximately equals J. The parameter a causes the dimensional value of R to range over $\pm 13\%$ within the weak and strong categories. (R is scaled by a^{-1}.) The dispersion of values caused by the range of a is modest and does not alter the qualitative results of this study. This dispersion is illustrated in Fig. 4. At $J = 2.7$, growth rates for $a\Lambda = 0.54$ with $n = 5$ and $a\Lambda = 0.45$ with $n = 6$ are both calculated.

The radial shear is a function of R (and r) as can be seen in (2) and by recalling that the basic state velocities are geostrophic. As noted above, there is weak variation in R (and r) for different wavenumbers J in order to have a continuous spectrum. Yet, the radial shear for the high and low curvature experiments is *identical* at any wavenumber J. So, while Λ is twice as large for low curvature, in (2) the factor $(r - R)$ is half as large due to the a^{-1} scaling of horizontal lengths. As noted before, the vertical shear is identical for all cases. This guarantees that the effects seen are due to curvature of the flow, and *not* to a change in the radial (cross-flow) or vertical shear.

Growth rate spectra for the two categories are plotted in Fig. 4. These rates are calculated using the bottom surface amplitude of the converged

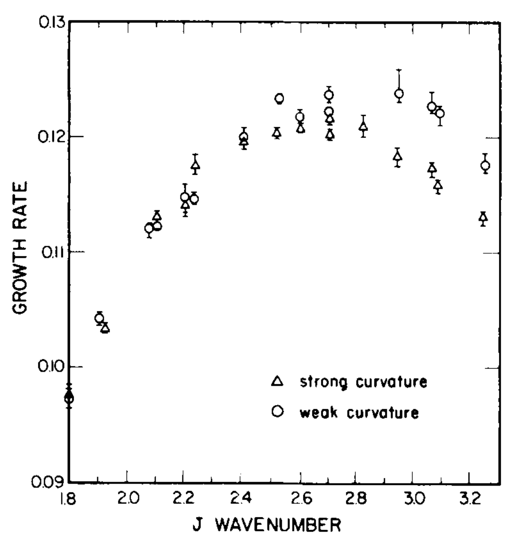

Fig. 4. Growth rate spectra for the weak (circles) and strong (triangles) curvature categories. Curvature reduces the short-wave ($J > 2.4$) growth rates. Two pairs of values are shown at $J = 2.7$; the lower of each pair is for $a\Lambda = 0.45$; the upper of each pair is for $a\Lambda = 0.54$; see text for more details.

eddy fields at intervals of fifty time steps. (The calculation assumes that the eddies are exponentially growing. If A_I is the initial amplitude and A_F is the amplitude after the passage of time Δt, then the growth rate equals $\Delta t^{-1} \ln [A_F A_I^{-1}]$.) There is some error in this calculation, so five rates are computed for each integration. The range of the five values is indicated by a vertical bar, with most values being close to that marked by a symbol. There is also some dispersion introduced by the range of a.

There are several comments that can be made regarding the growth rate spectra. The maximum growth rate occurs in the vicinity of $J \cong 2.7$. This is a somewhat shorter wavelength than is found for a straight, horizontally uniform flow with the same vertical structure. It is possibly an analogue of the well-known result for a straight flow: that the presence of cross-flow shear can preferentially destabilize the short waves (e.g., Simmons, 1974, or Grotjahn, 1980). The spectra for the strong and weak curvatures are most clearly different for the short waves ($J > 2.4$). *The stronger curvature causes a reduction of the short-wave growth rates.* This seems to contradict what one might extrapolate from Drazin (1978). Drazin formulated the Eady (1949) problem in approximately cylindrical coordinates and calculated neutral stability curves. This cylindrical geometry caused the neutral curves to shift in a manner which expanded the range of unstable waves. From this result one might argue that curvature would tend to increase instability. However, the opposite conclusion can be drawn from Fig. 4. This seeming contradiction will be resolved later, when the energy conversions are examined. In contrast to the short waves, the amount of curvature does not visibly alter the growth rates of the intermediate waves ($1.8 < J \leq 2.4$). This could be a product of how the basic state was chosen and will be addressed after the energy conversions are discussed, as well. There is some indication that the most unstable wave has a longer wavelength as the curvature increases. But, this may be just an artifice of the dispersion of data points mentioned above, instead of a real consequence of curvature.

Variation of the Coriolis parameter can influence whether eddies embedded in a given mean flow amplify or decay by the barotropic mechanism. (See discussion in Grotjahn, 1979; pp. 2062–2063.) The results from straight flow studies suggest that only the middle wavelength eddies might amplify by the barotropic mechanism if this problem were formulated with a linearly varying Coriolis parameter (i.e., on a "β-plane"). For analogous straight flows on a β-plane, the short waves are still barotropically damped; this implies that our basic result may not be changed if a more realistic Coriolis parameter is used.

A flavor for the structure of the eddies is obtained from Fig. 5. The figure shows the converged structure of the strong curvature solution for $J = 2.6$. On the left is a contour plot of the surface eddy pressure pattern; on the right are vertical profiles of the eddy pressure amplitude and phase at radius R. Vertical profiles from the initial field are included as well. It is clear that the vertical structure of the eddies for straight flow and no horizontal shear (the initial structure) is not changed much when curvature is added (the converged structure). The only notable difference is a tendency for the trough and ridge lines to be shifted further back (upstream) at high levels for the cylindrical mean flow. This result lends credence to the use of an initial field based upon an eigenfunction of comparable wavelength obtained for a straight flow of identical vertical shear but without horizontal shear (or curvature). The amplitude has relative maxima at the bottom surface and in the upper troposphere. The upper maximum occurs at somewhat higher altitude than initially. The phase shift (upstream with height) is indicative of baroclinic energy conversion and is slightly greater in the lower troposphere than initially. For shorter waves (not shown) the upper level amplitude becomes lessened and the waves are more bottom trapped, as found for comparable straight flows. Some of the differences may also be explained, in part, by computational limitations of the prognostic model.

Altogether, curvature did not materially alter the vertical structure of the eddies. However, it does significantly alter the horizontal structure. In Fig. 5, the horizontal structure shows eddies which have similar radial and longitudinal length scales, as desired. The longitudinal scale is assigned and the radial scale is dictated by the radial shear pattern in the basic state (see Simmons, 1974, or Grotjahn, 1979, for examples). That radial pattern was chosen to intentionally make the two horizontal scales nearly the same. Compared with the initial field (Fig. 3), the converged solution has developed radial tilts of the trough and ridge axes. By

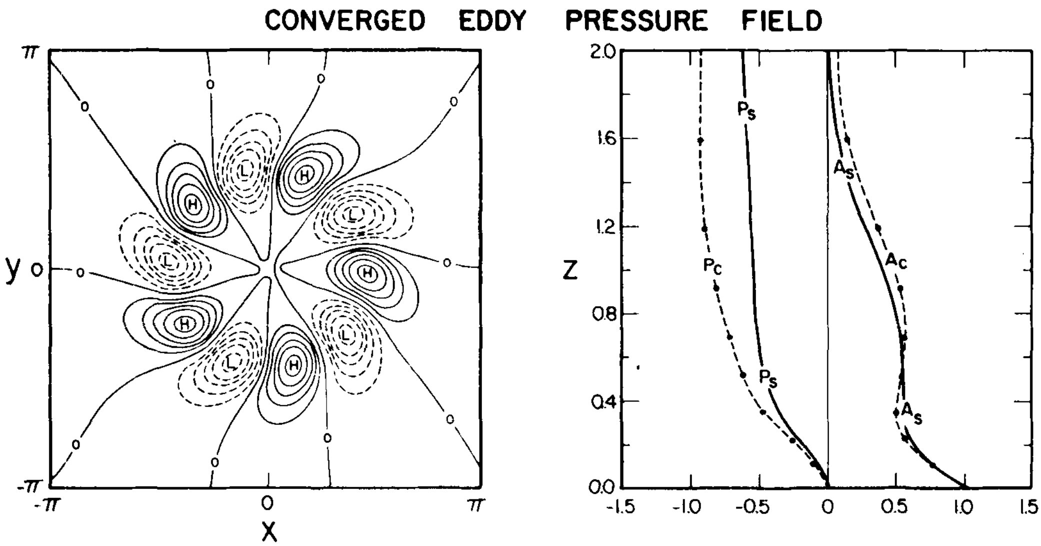

Fig. 5. Typical structure of the converged eddy fields; the format is similar to Fig. 3. A_c and P_c refer to the converged vertical profiles of amplitude and one-half phase angle at radius R. A_s and P_s are the corresponding profiles for a similar wavenumber where the basic flow has the same *vertical* structure, but is straight and without horizontal shear.

inspection, it appears that these tilts are indicative of barotropic energy conversion *from* the eddy *to* the mean flow. That will be demonstrated next.

The energy conversions are obtained by deriving a linearized version of the quasi-geostrophic perturbation energy equation. To isolate the energy conversion from the advective terms, appropriate spatial integrations (or averages) are made. For the straight zonal flows which have been analyzed by many previous workers in the field, it is particularly simple; one averages in the zonal direction. For straight flows oriented in arbitrary compass directions, it is natural to perform the averaging along the direction of the mean flow. For straight flows whose direction changes with height (Brode and Mak, 1978, or Grotjahn, 1982) horizontal averaging in both directions is employed and the baroclinic energy conversion becomes the sum of two components:

$$\bar{T}_x \overline{u'T'} + \bar{T}_y \overline{v'T'}.$$

These components are formed from the dot product of the mean flow temperature gradient and the eddy heat flux. In other words, it is a measure of the eddy heat flux directed orthogonal to the mean flow. For straight flows with cross-flow horizontal shear, the energy conversions are often displayed as a function of the cross-flow and vertical variables. The same approaches can be straightforwardly applied to the problem at hand by taking advantage of the cylindrical symmetry of the basic flow. For computational simplicity, the basic and eddy fields are mapped onto a longitude (θ) versus radius (r) coordinate system. Integrated over one longitudinal wavelength, the baroclinic conversion can be expressed as

$$\varepsilon \rho_s \bar{U}_z \int_0^\lambda \phi_\theta \phi_z \, d\theta \tag{5}$$

and the barotropic conversion as

$$\rho_s \bar{U} \int_0^\lambda [\phi_r \phi_\theta]_r \, d\theta, \tag{6}$$

where $r\lambda$ is the longitudinal extent of one wavelength. Note that (5) and (6) are merely the cylindrical coordinate version of the standard quasi-geostrophic energy conversions. For mean flows with complicated structure in all three dimensions and particularly in the along-flow direction, the most useful display of the energy conversion is not so straightforward. Frederiksen (1980) suggests that the fluxes of heat and momentum will be dominated by the *non*-oscillatory component. The oscillatory portion due to the motion of the eddy relative to the complex basic flow was largely ignored by him. This method seems useful for a linear problem, but it is unclear whether it is a useful analytic tool for nonlinear equations or, for that matter, the atmosphere. This subject may be discussed further in a future article.

The eddy amplitude is normalized to be equal to one at the bottom in all the energy calculations. Using (5), the baroclinic energy conversions for some representative solutions are shown in Fig. 6. The maximum value occurs in the lower troposphere. The distribution is virtually the same for the strong and weak curvature cases. Clearly the baroclinic energy conversion does not explain the influence of curvature upon the short-wave growth rates. The corresponding barotropic energy conversions calculated using (6) are presented in Fig. 7. Here there is a noticeable change brought about by the curvature. In all cases shown, there is a region of positive conversion for $r < R_c$ and a region of negative values for $r > R_c$. The cross-over radius R_c, where the conversion is zero, is slightly greater than R. Therefore, in all cases the eddies are tending to *increase* the radius of curvature of the mean flow. The eddies tend to reduce the basic flow for $r < R_c$ and increase it for $r > R_c$. When the curvature is weak there is an approximate balance between the two regions so that the net barotropic conversion is zero. For weak curvature, the distribution is nearly symmetric about R_c; for strong curvature it is not. When the curvature becomes strong the negative values of barotropic conversion become much larger than the positive. The net barotropic conversion is from the eddy to the basic flow. So, strong curvature barotropically damps the eddies. This explains why the short-wave growth rates are reduced when the curvature increases. Since the same barotropic conversion asymmetry occurs for the intermediate waves, it seems fair to ask why their growth rates are not altered by the curvature as well. The answer apparently lies in the choice of the basic state. Choosing the radial structure of the basic state so that the eddies develop comparable radial and longitudinal scales means that the radial shear is much weaker for the intermediate waves than for the short waves. Hence the barotropic instability mechanism is weaker for the intermediate waves. Even though the magnitude of the energy conversion in Fig. 6 for the $J = 2.1$ wave is larger than for $J = 3.06$, the total energy of the $J = 2.1$ wave is *much* larger still than that for $J = 3.06$. This is because the short waves are strongly bottom-

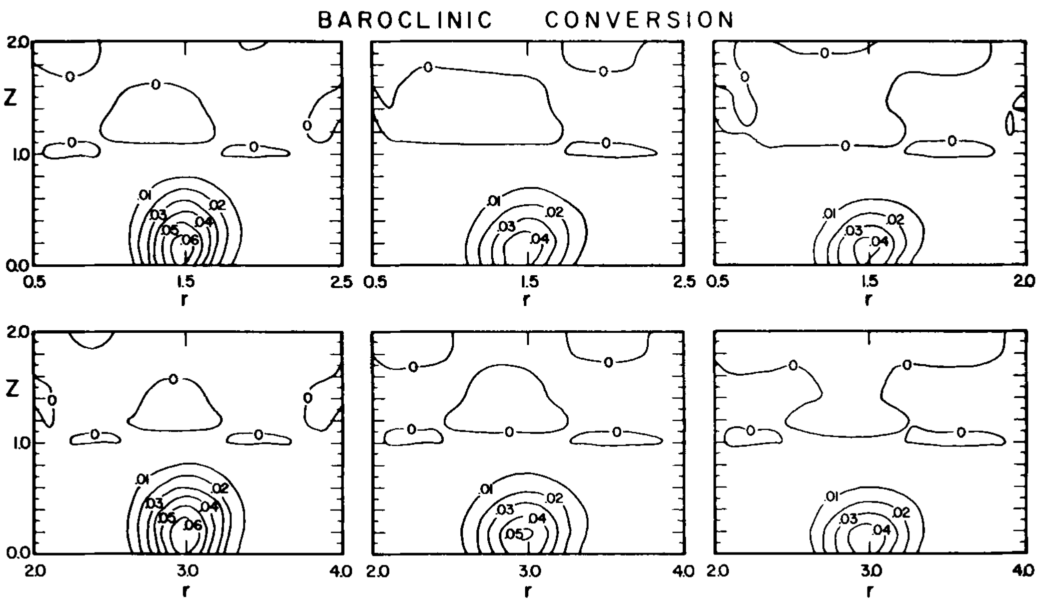

Fig. 6. Baroclinic energy conversions as a function of r and z. The upper diagrams are for strong curvature, the lower diagrams are for weak curvature. The left-hand plots are for $J = 2.1$ (an intermediate wave), the middle plots are for $J = 2.6$ (the most unstable wave) and the right-hand plots are for $J = 3.06$ (a short wave). Curvature hardly affects this conversion. The contour interval is 0.01 in the plots.

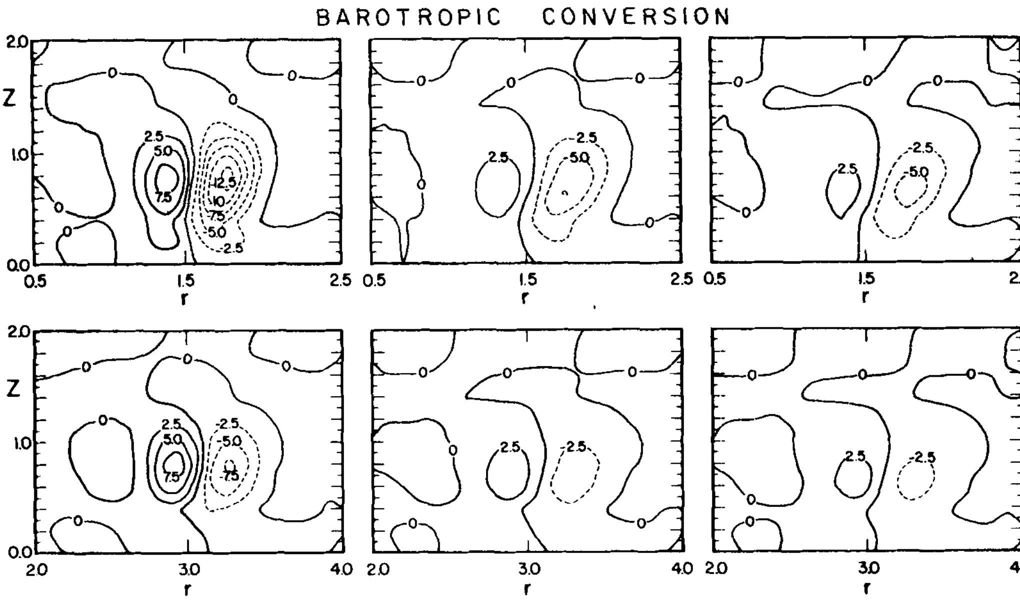

Fig. 7. Barotropic energy conversions for the examples shown in Fig. 6. Negative conversion is from the eddy to the mean flow. These plots imply (1) that strong curvature causes negative conversion and so lowers the growth rates and (2) that the eddies tend to increase the radius of curvature of the jet. The contour interval is 2.5×10^{-4} in all the plots.

trapped. Recall that the growth rate is proportional to the net energy conversions divided by the total eddy energy. Hence the intermediate wave growth rate is not affected as much by the barotropic mechanism as is the short-wave growth rate. Note that the magnitude of the baroclinic conversion significantly exceeds that of the barotropic conversion. Reexamining Fig. 4, we can see some slight suggestion that the growth rates are reduced by curvature for the intermediate waves. The effect is small for the longer wavelengths and is largely hidden by the dispersion of data points. Thus strong curvature induces negative barotropic energy conversion for *all* wavelengths presented. It would be visible as unambiguous reductions of the intermediate wave growth rates if the radial shear was increased by reducing the width of the basic flow jet. The intermediate waves would then have smaller radial widths, however.

It is useful to compare our results with those of previous studies which include some curvature in the mean flow. The comparison is useful to establish consistency between the various theoretical results. It is also useful to illuminate how our results (obtained for an idealized cylindrical mean flow) relate to more realistic wave-like mean flows and ultimately to geophysical flows. As stated in the introduction, this study considered an idealized flow just for this purpose: to isolate the role of curvature in complex flows.

Comparing the results here with those found for studies of wave-like mean flows is difficult; the wave flow results are dominated by effects due to along-flow variation. Additionally, the studies by Frederiksen are formulated in spherical geometry making comparison even more awkward, especially for the momentum fluxes (Hollingsworth, 1975). Recall that our results are for an f-plane. A direct comparison of the growth rates may not be feasible because the mean flows examined by others had different cross-flow structure and the jet was centered at a different latitude as the curvature changed. However, the eddy spatial structure and, more appropriately, the eddy energy conversions might be profitably compared.

Given this caveat, let us examine some representative results from Frederiksen (1980). Frederiksen finds the "nonoscillatory" baroclinic energy conversion to be predominately positive and centered close to, but possibly shifted to the smaller radius of curvature side of the jet. There is some corresponding indication in Fig. 6 that the baroclinic conversion is a maximum at a radius slightly less than R. Frederiksen finds that his eddies develop cross-flow horizontal tilts indicative of barotropic energy conversion; his eddies appear damped by this mechanism. This also agrees with the results here. His eddy momentum fluxes tend to be strongest where the flow is both swift and curved (relative to latitude and longitude lines). Some care is required when comparing the horizontal structures; this is illustrated by two of his cases. For his 39° jet (see his Fig. 6), the nonoscillatory barotropic conversion has a bi-polar structure about the jet: with negative values to the poleward side and positive values equatorward. Superficially, this seems to be the reverse of the pattern in Fig. 7 since Frederiksen's greatest eddy momentum convergence is located near the entrance region to the long-wave trough. Just upstream, near the ridge, is where his "excess" vertical shear (and hence the instability) is greatest. Around the *ridge* his bi-polar pattern *agrees* with Fig. 7; mainly negative values of nonoscillatory barotropic conversion occur for a larger radius of curvature than the jet and positive values at a smaller radius. So, his eddy momentum flux is distributed in a fashion which implies that the eddies are tending to make the mean flow more zonal, but at a *higher latitude*. For his 30° jet (see his Fig. 5), the nonoscillatory barotropic conversion apparently has only a slight bi-polar structure about the jet. To the extent that it exists, there is some suggestion that positive values occur poleward and negative values equatorward of the jet in the entrance region of the long-wave ridge. Just upstream, near the trough, is where the excess shear is greatest in this case. So again, close inspection reveals that there is a tendency for the eddies to straighten out the jet, but now towards a zonal flow at a *lower latitude*. The tendency toward reducing the mean-flow curvature is consistent with the results presented here despite the shortcomings of the comparison. Note that Hollingsworth (1975) compared eigenmodes for solid body rotation on a sphere with those for horizontally uniform mean flow on an f-plane. Hollingsworth found a net poleward momentum convergence on the sphere while there was none on the f-plane. For convenience, let's refer to the eddy momentum flux induced by the spherical geometry as a "geometric flux". The geometric flux may explain some of the asymmetry in Frederiksen's figures. For the 30° jet there is some tendency for the curvature induced flux to be directed counter to the geometric flux and thus the nonoscillatory flux in his Fig. 5 has a complicated spatial pattern. For the 39° jet there is some tendency for the curvature and geometric induced fluxes to constructively add, and thus the nonoscillatory flux tends to be mainly of one sign and more simply distributed.

Finally, there seems to be a correspondence between the latitude of the greatest excess shear and the latitude of the more zonal mean flow deduced from the eddy momentum conversion. The mechanism is presumably related to the fact that just downstream of the area of greatest excess shear, the eddies are generally largest in amplitude; their fluxes therefore tend to be larger there[2]. This raises an interesting question. Can a curved mean flow be maintained when there is a rough balance between the excess shear at the trough and that at the ridge? In this situation neither area of enhanced eddy development would predominate, and hence the mean flow might not be forced toward a more zonal flow at only one latitude. Of course, this is speculation, but it may help elucidate how curving geophysical flow patterns might be maintained in the presence of growing eddies. Prime examples of such curving flows are the persistent midlatitude blocking patterns.

4. Summary

This has been the third report in a series devoted to isolating special cases of the linear stability problem for complicated three-dimensional time-mean flows. The hope has been that analyses of the more easily understood special cases could be used to improve our understanding of the more general problem. The two prior papers considered arbitrary compass orientation (the role of β) and turning of the wind with height, respectively. In this paper, the effect of horizontal curvature of the steering flow

[2] This displacement occurs because while the eddy grows fastest in the region of excess shear, it reaches its "largest" amplitude slightly downstream because it moves with the flow as it grows. This is the only mechanism by which Frederiksen's growth rates can have spatial variability; the eddies can be thought of as moving through an amplitude envelope which is fixed with respect to the long wave.

was examined employing cylindrically symmetric basic flows on an f-plane.

The experiments were stratified according to wavenumber and according to whether the curvature was strong or weak. The *radius* of maximum basic state velocity, R, was twice as large for the weak as it was for the strong curvature. In all other respects, the basic flows were essentially the same. Most earlier papers posed the equations as eigenvalue problems. Here, a prognostic model was used because it has several advantages for this non-separable problem. The initial conditions were derived from a combination of analytic functions (for the horizontal structure) and eigenfunctions (for the vertical structure). The latter were derived from a simpler, separable version of this problem.

The major effect of curvature was to reduce the short-wave growth rates. The reduction was caused by the barotropic energy conversion mechanism. Actually, the barotropic conversion was negative, that is, directed from the eddy to the mean flow, for *all* wavelengths when the curvature was strong. Only for the short waves was this conversion strong enough to significantly reduce the growth rates. This may result from choosing the basic state so that it makes the longitudinal and radial length scales of the eddies approximately equal. This meant that the radial (cross-flow) shear must be much stronger for the short waves than for the intermediate waves. Consequently, one anticipates that the barotropic conversion mechanism may have been enhanced for the shorter waves. If only the radial shear is increased, it seems likely that the intermediate waves would be noticeably damped by strong curvature as well, at least, on an f-plane. However, previous work with straight flows (Grotjahn, 1980, for example) has shown that the stronger cross-flow shear will shift the most unstable wavelength to a shorter value. This was shown for both f-plane and β-plane solutions. Apparently, stronger radial shear increases the barotropic damping of the short waves more strongly when the mean flow is curved than it does when the mean flow is straight.

In all the cases examined there was a tendency for the barotropic conversion to be positive for radii less than R and negative for radii larger than R. The eddies developed radial tilts of the trough and ridge axes accordingly. This means that the eddies had a propensity to weaken the basic flow for radii less than R and strengthen it for larger radii, to increase its radius of curvature. In other words, *the eddies tended to straighten out the mean flow.* For weak curvature, the positive and negative areas of conversion nearly compensated. For strong curvature the negative area dominated.

Several properties of the waves were little changed by the basic flow curvature. The eddies remained principally baroclinically energy-converting. This conversion appeared to be hardly influenced by the strength of the curvature. It was largest in the lower troposphere. The amplitude profile and upstream phase shift with height also seemed insensitive to the curvature. They remained quite similar to the initial guess vertical structure, thus vindicating the initialization procedure used.

A comparison was made with the results obtained by others who examined long-wave basic flows. Frederiksen (1980) was used as a representative example. It was shown that, despite difficulties in comparing the models and basic flows, there is some agreement between the present and previous studies. In reexamining Frederiksen's results, it was found that the eddies tended to make the basic flow more zonal but that the central latitude of the new (more zonal) basic flow seemed linked to the latitude of the most unstable region of the basic flow. The question was raised of whether a curved mean flow might be *maintained* by the eddies if there were two regions of approximately equal instability occurring at different latitudes. It was speculated that such a simple linear mechanism might maintain persistent atmospheric features such as a blocking pattern. This question will receive further consideration in a forthcoming article.

5. Acknowledgements

I wish to thank G. Branstator, R. Daley and J. Tribbia for giving their time to assist me in this research. I also thank P. Thompson for some useful comments. This work was initiated while the author was a postdoctoral fellow at the National Center for Atmospheric Research (NCAR). The research was completed while the author was a visiting fellow at the Cooperative Institute for Research in Environmental Sciences (CIRES). NCAR is sponsored by NSF; CIRES by NOAA. The manuscript was typed by C. Winkler (CIRES), and P. Laugenour (Univ. of Calif., Davis); the figures were drafted by R. McDonald (CIRES).

6. Appendix

a	horizontal length scaling parameter
D	vertical length scale [$=10$ km]
f_0	constant Coriolis parameter
g	acceleration of gravity
J	longitudinal wavenumber (dimensionally scaled)
L	Rossby radius of deformation at surface: horizontal length scale (~ 1100 km)
N	number of waves around circle of radius R
q	quasi-geostrophic potential vorticity
$\bar{q}_x, \bar{q}_y$	basic state potential vorticity gradient components
r	radial coordinate
R	radius of maximum basic flow
t	time
$\bar{U}, \bar{V}$	x, y components of basic flow
x	eastward coordinate
y	northward coordinate
z	vertical coordinate
β	first meridional derivative of f
ε	$(=f_0^2 L^2/g\kappa D)$
θ	longitudinal coordinate
κ	horizontally averaged static stability
Λ	strong, weak curvature parameter [$=1, 2$]
ρ_s	horizontally averaged density
Ω	[$=(\ln \rho_s)_z$]
ϕ	eddy pressure

REFERENCES

Baines, P. G. 1976. The stability of planetary waves on a sphere. *J. Fluid Mech. 73*, 193–213

Brode, R. W. and Mak, M. 1978. On the mechanism of the monsoonal mid-tropospheric cyclone formation. *J. Atmos. Sci. 35*, 1473–1484.

Coacker, S. A. 1977. The stability of a Rossby wave. *Geophys. Astrophys. Fluid Dyn. 9*, 1–17.

Drazin, P. G. 1978. Variations on a theme of Eady. In *Rotating fluids in geophysics* (eds. P. M. Roberts and A. M. Soward). London: Academic Press, 154–163.

Eady, E. T. 1949. Long waves and cyclone waves. *Tellus 1*, 33–52.

Egger, J. 1969. The development of cyclone waves at a stationary, longwave basic state. *Beitr. Phys. Atmos. 42*, 174–191.

Frederiksen, J. S. 1978. Instability of planetary waves and zonal flows in two-layer models on a sphere. *Quart. J. Roy. Meteorol. Soc. 104*, 841–872.

Frederiksen, J. S. 1980. Zonal and meridional variations of eddy fluxes induced by long planetary waves. *Quart. J. Roy. Meteorol. Soc. 106*, 63–84.

Gill, A. E. 1974. The stability of planetary waves on an infinite beta-plane. *Geophys. Fluid. Dyn. 6*, 29–47.

Grotjahn, R. 1979. Cyclone development along weak thermal fronts. *J. Atmos. Sci. 36*, 2049–2974.

Grotjahn, R. 1980. Linearized tropopause dynamics and cyclone development. *J. Atmos. Sci. 37*, 2396–2406.

Grotjahn, R. 1981. Stability properties of an arbitrarily oriented mean flow. *Tellus 33*, 188–200.

Grotjahn, R. 1982. Stability properties of mean flows with turning. *Tellus 34*, 39–49.

Hollingsworth, A. 1975. Baroclinic instability of a simple flow on a sphere. *Quart. J. Roy. Meteorol. Soc. 101*, 495–528.

Hoskins, B. J. 1973. Stability of the Rossby-Haurwitz wave. *Quart. J. Roy. Meteorol. Soc. 99*, 723–745.

Kim, K. 1978. Instability of baroclinic Rossby waves; energetics in a two-layer ocean. *Deep Sea Res. 25*, 795–814.

Lorenz, E. N. 1972. Barotropic instability of Rossby wave motion. *J. Atmos. Sci. 29*, 258–264.

Niehaus, M. C. W. 1980. Instability of non-zonal baroclinic flows. *J. Atmos. Sci. 37*, 1447–1463.

Simmons, A. J. 1974. The meridional scale of baroclinic waves. *J. Atmos. Sci. 31*, 1515–1525.